Polymer-stabilized cholesteric liquid crystals as switchable photonic broad bandgaps

Michel Mitov, E. Nouvet, N. Dessaud

Accepted version published in: *Eur. Phys. J. E*, **15**, 413-419 (2004).

Polymer-Stabilized Cholesteric Liquid Crystals as switchable photonic broad-bandgaps

Michel Mitov•, Emmanuelle Nouvet and Nathalie Dessaud

Centre d'Elaboration de Matériaux et d'Etudes Structurales, CEMES–CNRS

29 rue Jeanne-Marvig, BP 94347

F-31055 Toulouse cedex 4, France

email : mitov@cemes.fr

Article history: Received 13 July 2004 / Published online: 7 December 2004.

https://doi.org/10.1140/epje/i2004-10058-4

• corresponding author

Accepted version published in: *Eur. Phys. J. E*, **15**, 413-419 (2004).

A cholesteric liquid crystal can be considered as a one-dimensional photonic crystal with a refractive index that is regularly modulated along the helix axis, because of the particular arrangement of the molecules. The result is that the propagation of light is suppressed for a particular range of wavelengths (bandgap). A Polymer-Stabilized Cholesteric Liquid Crystal, which is obtained by in-situ photopolymerization of reactive liquid crystal molecules in the presence of non-reactive liquid crystal molecules in an oriented Bragg planar texture, is elaborated by combining the UV-curing with a thermally-induced pitch variation. As a consequence, it is shown here that memory effects are introduced into the characteristics of the reflection band of the material at room temperature. In the visible spectrum, the reflection bandwidth can be tuned in agreement with the thermal ramp and broadened. In addition, the bandgap filters can be switched between broadband reflective, scattering and transparent states by subjecting them to an electric field. Related application fields of these functional materials are switchable smart windows for the control of solar light spectrum and white-or-black polarizer-free reflective displays.

1. Introduction

1.1. Bragg reflection in cholesteric liquid crystals

Photonic crystals that have an ordered structure with a periodicity of an optical wavelength have attracted considerable attention from both fundamental and practical points of view, because novel physical concepts such as the photonic bandgap have been theoretically predicted and various applications have been proposed. Photonic bandgap materials present potential applications in display technology, telecommunications and fiber optics[1, 2]; in addition, organic materials are promising for photonics because of the versatility in molecular design: relative ease of synthesis, characterization and processing. A cholesteric liquid crystal (CLC) can be considered as a one-dimensional photonic crystal with a refractive index that is regularly modulated along the helix axis, because of the particular arrangement of the molecules. The result is that the propagation of light is suppressed for a particular range of wavelengths. The wavelength region in which the light can not propagate is the stop band, which is another representation of the selective reflection band and is considered as a one-dimensional pseudo-bandgap. Such Bragg reflections are exhibited by a CLC slab with a uniformly oriented Grandjean planar texture (*i. e.* the helix axis is perpendicular to the observation plane)[3]. At normal incidence, the central wavelength lambda of the stop band $\bar{\lambda}$ is related to the cholesteric pitch p and the mean refraction index $\bar{n}$ by:

$$\bar{\lambda} = \bar{n}\, p.$$

$\bar{n}$ is the average of the ordinary (n_o) and extraordinary (n_e) refractive indices of the locally uniaxial structure: $\bar{n} = (n_o + n_e)/2$. The spectral width of the stop band $\Delta\lambda$ is defined as:

$$\Delta\lambda = p\,\Delta n$$

where $\Delta n = n_e - n_o$ is the birefringence. Within $\Delta\lambda$, an incident unpolarized or linearly polarized light beam parallel to the helix axis is split into two opposite circularly polarized components, one of which is transmitted whereas the other is totally reflected. The sense of rotation of the latter one agrees with the helix screw sense. A wavelength out of $\Delta\lambda$ is simply transmitted. Compared to conventional pigmented color filters, a CLC filter has the advantage to integrate several optical properties in one layer: it is not only a color filter but also a reflector and a polarizer. Since Δn values are limited for colourless organic compounds, $\Delta\lambda$ is often less than 100 nm in the visible spectrum.

1.2. Polymer-Stabilized Liquid Crystals: principles

Polymer-Stabilized LCs (PSLCs) or anisotropic gels are composite materials made of a crosslinked LC polymer and nonreactive low molar mass LCs (LMMLCs) like cyanobiphenyl mixtures[4]. These materials are produced by the *in situ* UV-polymerization of a few weight percent of LC monomers in the presence of the LC solvent. Depending on the pitch range, PSCLCs exhibit specific optical and electro-optical properties which give rise to bistable reflective displays or light shutters with normal and reverse modes[5]. The introduction of memory effects by the presence of polymer network in relation with the elaboration conditions of the composite material are of paramount importance. In the case of cholesteric gels subjected to an electric field, the network can aid in the return of the initial LC director orientation and reduce the switching time for polymerization in the Grandjean texture[6]. For nematic gels cured in the nematic phase, a paranematic order in the LC in the isotropic phase induced by the network surfaces has been evidenced[7]. The fact of increasing the temperature range for the properties is relevant for device applications[8].

1.3. Objectives of the work

We investigate at room temperature the behaviour of the reflection band of cholesteric gels which were elaborated during a temperature ramp, which corresponds to a continuous pitch variation. In relationship with potential memory effects, the underlying question is: Do the reflection characteristics of the composite material at room temperature integrate the color changes which occurred during the in situ network formation ? We expect from such modus operandi the realization of switchable photonic bandgap materials exhibiting an enlarged reflection bandwidth when common CLCs have a narrow bandgap due to a low or medium birefringence.

2. Experimental

Materials: A photocrosslinkable CLC, RM9 (from Wacker Chemie Ltd.), is blended with a LMMLC mixture. RM9 is a mesomorphic oligomer suited for the production of optical filters and consists of a mixture of reactive monomers and side groups LC polymers with a siloxane backbone[9]. An amount of 2 wt. % (compared to RM9 concentration) of photoinitiator Irgacure 907 (from Ciba-Geigy) is added. The LMMLC is a blend of BL087, BL088 and CB15 mixtures from Merck Ltd. The concentration (in wt.%) is as follows: 70 [82 BL088 + 18 CB15] + 30 BL087. In the final blend, the concentration in network-forming material (RM9) is 3.85 wt.%.

Cell characteristics: The blend is introduced at 50°C by capillarity in a 15 μm (± 3 μm) thick ITO-glass cell (from EHC CO. Ltd., type FF). In order to induce a planar orientation the

surfaces were treated with rubbed polyimide (the plates are assembled with their rubbing directions making an angle of 180°).

UV-curing conditions (Figure 1). The cell is firstly stabilized at the aimed temperature during 15 minutes for the purpose of LC alignment. The sample is then UV-cured at 365 nm with a power of 0.1 $mW.cm^{-2}$ (measured with a radiometer, UVR-365 from Prolabo). Finally, the cell comes back to room temperature via a ramp with a speed equal to 2°C/min.

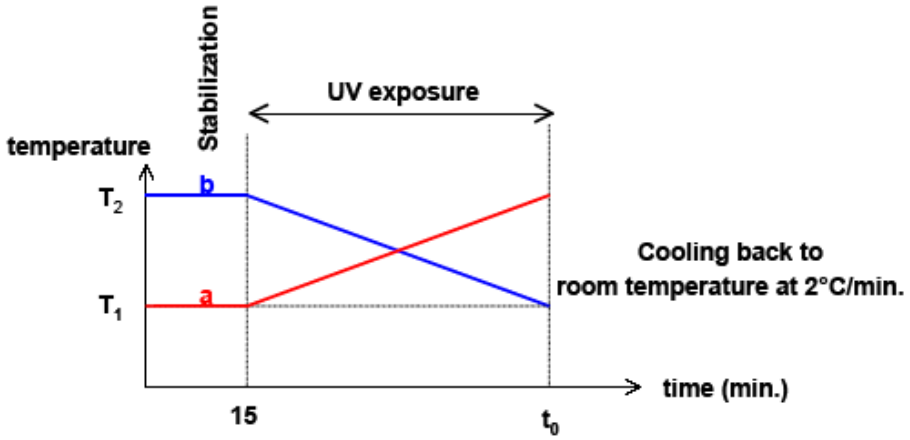

FIGURE 1. Principle scheme of thermal and curing processes in the case of a ramp. Three steps: stabilization of liquid crystal alignment during 15 min.; UV-exposure during: (a) an increasing or (b) a decreasing ramp; cooling back to the room temperature at 2°C/min after UV-exposure.

Voltage characteristics: square-wave voltage, frequency : 1 kHz.

Transmittance spectra: The transmitted light intensity as a function of wavelength is investigated at room temperature (between 20 and 22°C) by unpolarized spectrophotometry (UV-3100 Shimadzu). It is checked that negative peaks are due to reflectance and not to absorbance. See Figure 2 for details on the measurements of parameters taken from transmittance spectra.

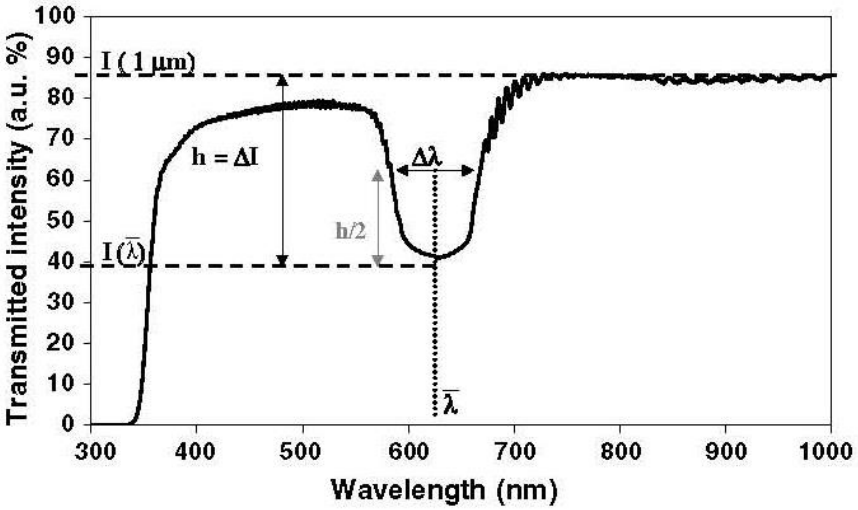

FIGURE 2. Representation of the different parameters extracted from a transmittance spectrum.

Material preparation for SEM investigations: The gel cell was plunged in liquid nitrogen and broken in a direction perpendicular to the plates. One of the two pieces was immersed in cyclohexane during 12 hours to dissolve out the LC and to leave the bare network architecture. After the solvent removal, the material was finally sputtered with a thin layer of gold. The transversal section was observed.

3. Results

3.1. Polymorphism of the cholesteric blend before curing

Grandjean planar textures were investigated by polarized-light microscopy between crossed polarizers when the temperature is increased from 22°C until the cholesteric–isotropic transition, which begins at 72°C (biphasic texture). Inside this range the reflection colour varies from orange to dark red; the texture micrographs were reported in a previous

paper[10]. The pitch variation with the temperature was investigated by using the Grandjean-Cano wedge method[11]. As displayed in Figure 3, the pitch varies from 420 to 530 nm when the temperature varies from 22 to 70.3°C.

The behaviours we report below have been reproduced on several other cyanobiphenyl mixtures; the milestone is the presence of a thermally-induced pitch variation of the CLC blend and not a peculiar chemistry of mesogens.

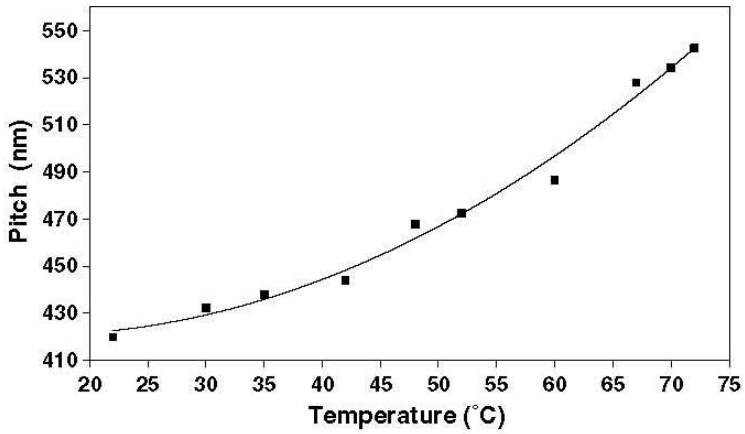

FIGURE 3. Helical pitch of the cholesteric liquid crystal blend vs. temperature before curing.

3.2. One-step processes: UV-curing at a single temperature

As an example, Figure 4 shows the variation of transmitted intensity as a function of the wavelength for cells before and after curing at 70.3°C during 30 minutes. Nearly 50% transmission comes from polarization selectivity; the sudden decrease of the transmittance below 400 nm is due to the cut-off wavelength for glass which affects the shape of cell spectra. Prior curing, $\bar{\lambda}$ is around 620-630 nm at 22°C and is kept rather constant after curing whereas the bandwidth $\Delta\lambda$ is modified as a consequence of such an out-of-equilibrium curing: $\Delta\lambda$ is increased from 80 to 175 nm.

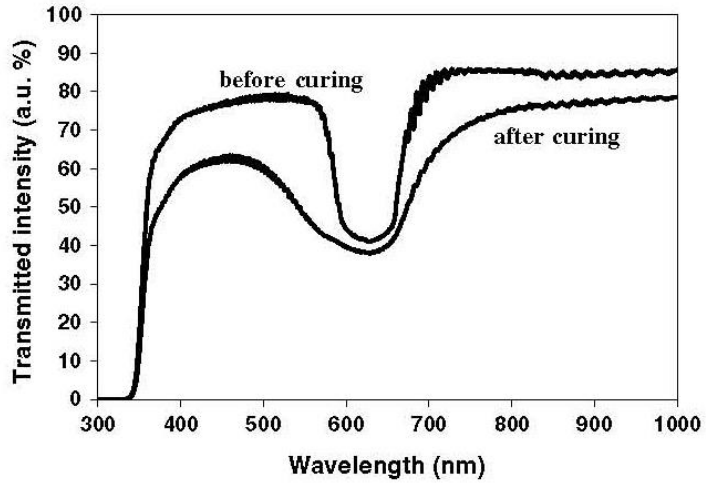

FIGURE 4. An example of transmittance spectrum before and after UV-curing (at 70.3°C during 30 minutes).

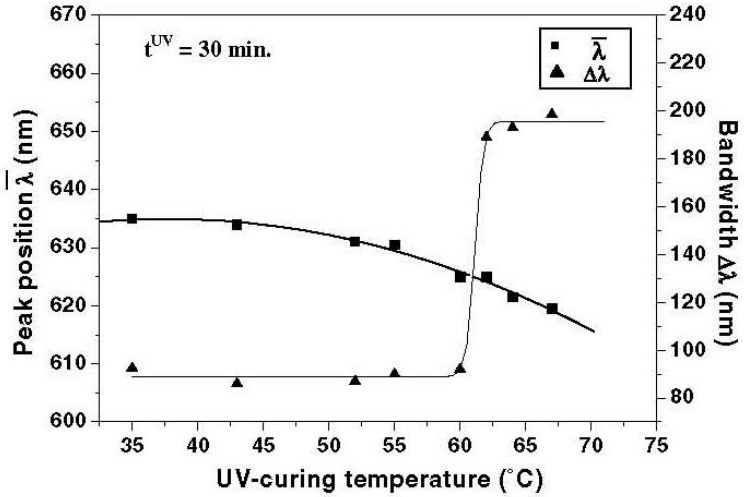

FIGURE 5. Central wavelength $\bar{\lambda}$ and bandwidth $\Delta\lambda$ of the stop band vs. curing temperature for one-step thermal processes.

Figure 5 shows the variation of the peak position $\bar{\lambda}$ and bandwidth $\Delta\lambda$ as a function of the curing temperature for a set of temperatures which belong to the forthcoming ramp and a curing time equal to 30 minutes. $\bar{\lambda}$ slightly decreases from 635 to 615 nm when the curing temperature is changed from 35 to 70.3°C. The behaviour of $\Delta\lambda$ is clearly different: $\Delta\lambda$ is constant (around 90 nm) up to 60°C, then undergoes a jump up to 190 nm and finally slightly

varies between 190 and 200 nm when the temperature is changed from 65 to 70.3°C. Increased values of $\Delta\lambda$ are therefore attached to the high temperature processes.

Figures 6.a and b show the variation of $\bar{\lambda}$ and $\Delta\lambda$ as a function of the curing time (between 15 and 110 minutes) for two temperatures – respectively 35.4°C and 70.3°C – which are the bounds of the forthcoming ramps; the positions of $\bar{\lambda}$ and $\Delta\lambda$ before curing are also indicated with dotted lines. When the material is cured at 35.4°C, $\bar{\lambda}$ as well as $\Delta\lambda$ are not significantly modified by the curing process for whatever curing time: $\bar{\lambda}$ and $\Delta\lambda$ are kept at respectively 630/635 and 90 nm. When the material is cured at 70.3°C, $\bar{\lambda}$ slightly decreases from 630 nm (before curing) to 620 nm whereas $\Delta\lambda$ is distinctly enlarged from 80 to about 190/200 nm. The time-dependence of $\bar{\lambda}$ and $\Delta\lambda$ is weak probably due to the fast achievement of the polymerization reaction by comparison with the present time scale of investigation.

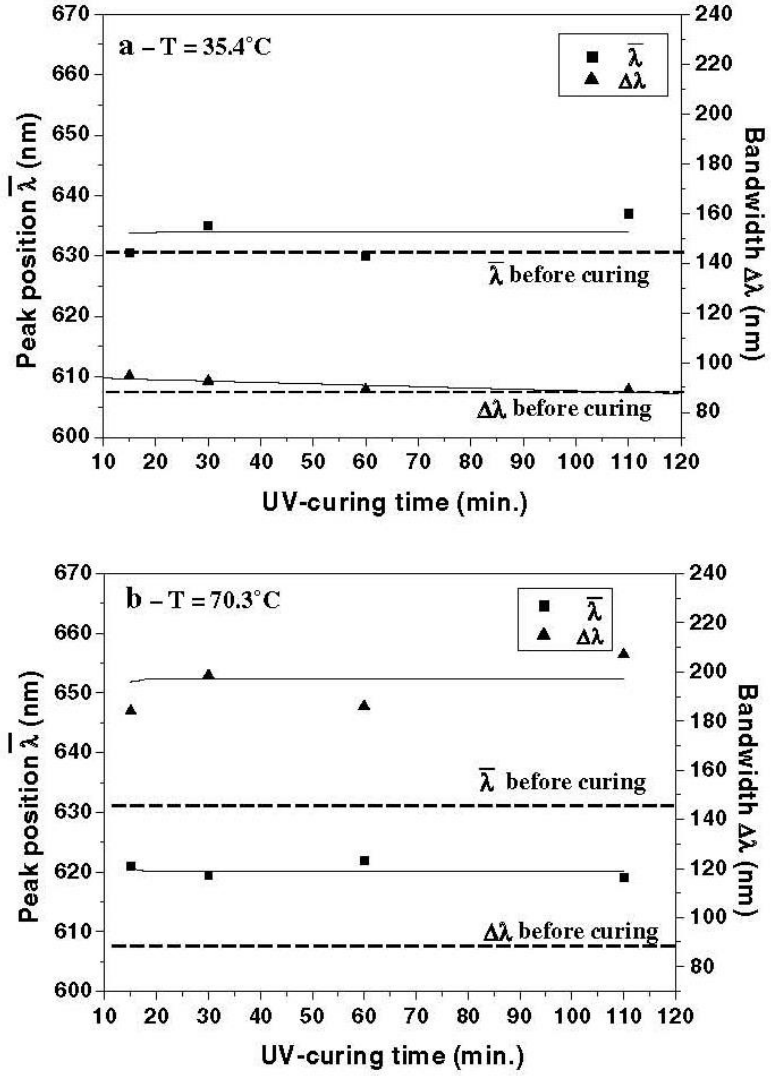

FIGURE 6. Central wavelength $\bar{\lambda}$ and bandwidth $\Delta\lambda$ of the stop band vs. curing time when the curing temperature was equal to: (a) 35.4°C and (b) 70.3°C. Dotted lines correspond to the values before curing.

In summary on one-step processes: $\bar{\lambda}$ is not significantly modified by the curing temperature and time whereas $\Delta\lambda$ is enlarged above a critical temperature (> 60°C) and the behaviour is time-independent.

3.3. Continuous processes: UV-curing during a thermal ramp

The purpose to investigate the role of a continuous pitch variation on the reflection properties during the UV-curing is almost twofold: *(i)* to discuss the occurrence of cumulative effects on the characteristics of the reflection band at room temperature; *(ii)* by investigating linear ramps with both senses (from low to high temperature and reciprocally): to study the influence of the pitch amplitude at the beginning of the formation of the network, which could be responsible for memory effects.

Figure 7.a shows the variation of $\bar{\lambda}$ and $\Delta\lambda$ as a function of the curing time (between 15 and 110 minutes) when the temperature continuously changes from 35.4 to 70.3°C. The behaviours are very slightly changed in comparison with those related to the curing at 35.4°C (Fig. 6.a) and are time-independent: $\bar{\lambda}$ and $\Delta\lambda$ are respectively around 635 and 90 nm. The situation is different when the ramp starts at 70.3°C as shown in Figure 7.b: $\bar{\lambda}$ decreases from 635 to 610 nm but especially $\Delta\lambda$ increases from 110 to 240 nm. Thus the effect of the ramp type on $\bar{\lambda}$ and $\Delta\lambda$ depends on the ramp slope (amplitude and sign). For ramps with positive slope (Fig. 7.a), the position and width of the reflection peaks are not affected by how fast the temperature increases during curing; for ramps with negative slopes (Fig. 7.b), the reflection peaks are strongly affected by the slope. For slower ramps (curing times higher) the reflection bandwidth is enlarged and a shift of the central wavelength lambda of the stop band to the lower wavelengthes occurs; however, there are almost no differences in value between a 60 and a 110 minutes exposure time: a plateau has been reached. To broaden the reflection band, it is thus necessary to expose for a sufficient amount of time (almost 35 minutes). These results agree with the hypothesis of a link between the broadening of the reflection peak and

the difference between the cholesteric pitches at the exposure and measurement (room) temperatures.

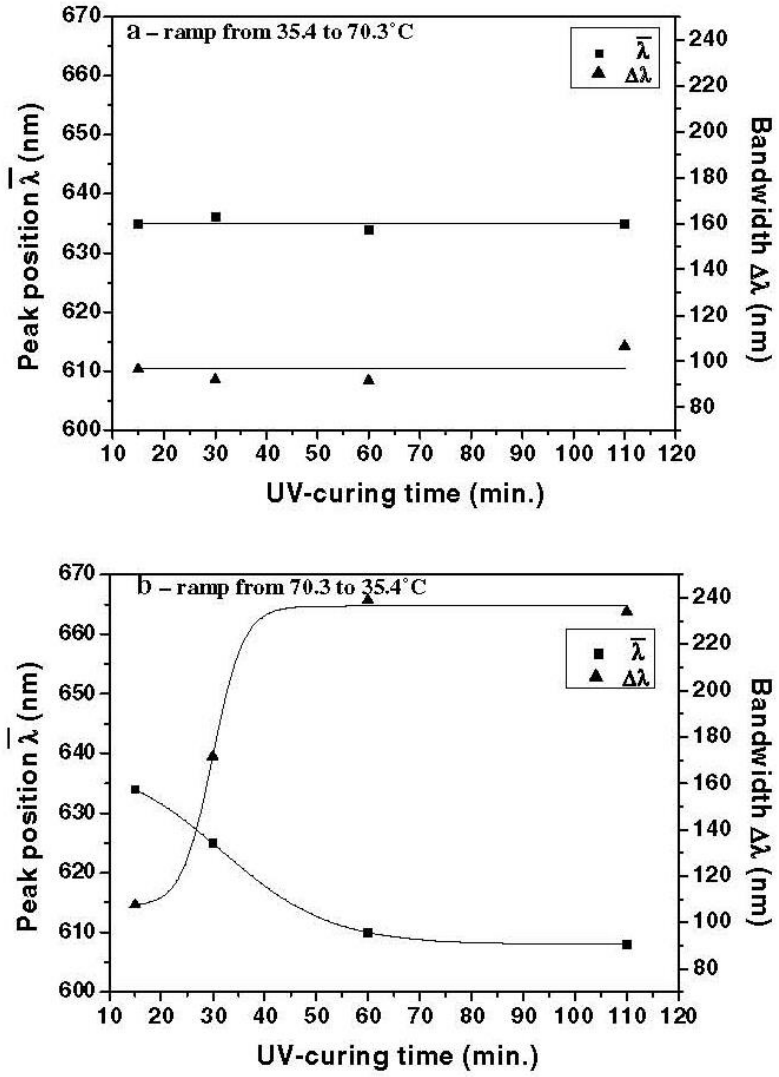

FIGURE 7. Central wavelength $\bar{\lambda}$ and bandwidth $\Delta\lambda$ of the stop band vs. curing time when the temperature was changed during a ramp: (a) from 35.4°C to 70.3°C or (b) from 70.3°C to 35.4°C.

Morphology of polymer network, as investigated by scanning electron microscopy (SEM), for the ramp starting at high temperature and during 110 minutes (Fig. 8) looks like an aggregation of small beads probably due to increased rate of initiation of

photopolymerization arising from additional initiation of polymerization due to thermal initiation at the highest temperatures. These patterns are consistent with morphologies previously observed in PSCLC[5.a, 12] or Polymer-Stabilized Nematic LCs[13].

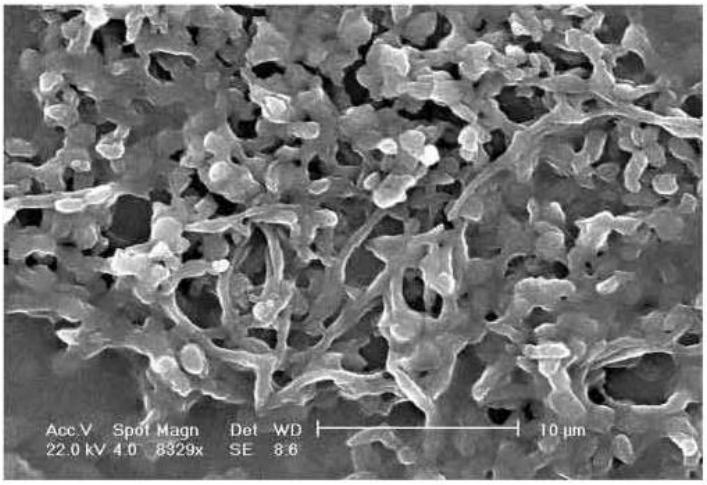

FIGURE 8. SEM micrograph of polymer network when the blend was cured during a ramp from 70.3°C to 35.4°C (time = 110 min.).

Figures 9.a and b show the variation of the I/I_0 ratio at $\bar{\lambda}$ and 1 µm as a function of the curing time for ramps of both senses (I_0 and I are the transmitted light intensities before and after curing; see §.2 and Figure 2 for details on the measurement of parameters peculiar to the transmittance spectra); the analysis of the evolution of the transmitted light intensity at 1 µm is relevant to follow the evolution of the mean level of the signal far from the reflection peak, and thus regardless of the mean level of the reflection peak. Both ratios slightly decrease between 90 and 80 % when the curing time increases from 15 to 110 minutes: the transmitted intensities are slightly affected by the curing process. Transmittance decreases are typical from the highest curing times and are due to a phenomenon of light scattering. The decrease of transmitted light intensity is more pronounced when the ramp starts at high temperature (Fig. 9.b): the high temperature curing process slows down the polymerization rate and may produce coarser polymer networks like in the case of nematic gels[14, 15], since the

temperature dependence of the diffusion coefficient is much stronger than that for the reaction rate. Coarser polymer networks produce larger microdomains inducing light scattering in the optical properties of the gel cell. Increasing the temperature of photopolymerization increases the size of the constituent units and correspondingly the size of the pores of the polymer network. This is due to the transition of aggregation behaviour from being reaction-limited at short length and time scales to being diffusion-limited at greater length and time scales; a model explaining the dependence of the characteristic dimension of the polymer network on the concentration and the relative rates of diffusion and reaction was developed on this topic[15].

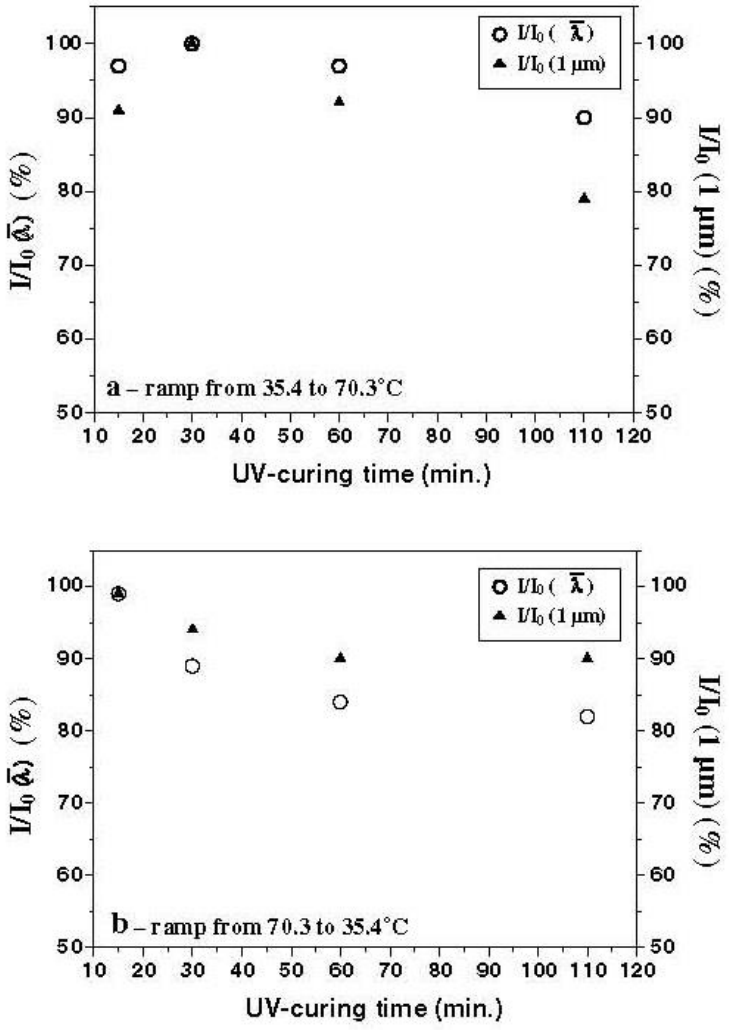

FIGURE 9. Transmitted intensities ratio at the central wavelength $\bar{\lambda}$ and at 1 μm vs. curing time when the temperature was changed during a ramp: (a) from 35.4°C to 70.3°C or (b) from 70.3°C to 35.4°C. I_0 and I are the intensities before and after curing.

We also investigated the variation of $\Delta I/\Delta I_0$ (where $\Delta I = I\ (1\ \mu m) - I\ (\bar{\lambda})$) as a function of the curing time for both ramps: the peak height is not significantly affected by the curing process ($\Delta I/\Delta I_0$ is kept between 95 and 100%).

3.4. Switchability of the broad-bandgaps

Finally, the switchability of cells is checked. Figure 10 shows an example of three typical states which are reached when a voltage is applied to the cell (in the case of a ramp from 70.3 to 35.4°C during 60 minutes). At zero volt or for very weak voltages, the cell exhibits a broadband reflection. Then the position as well as the bandwidth of reflection peak are modified and the cell changes from a reflecting to a scattering state (e.g.: 25 V). As in PSCLCs with a narrow band for reflection, light scattering is due to a focal conic texture exhibiting polydomains[16]. This is the result of a competition between LC molecules close to the polymer network which have a tendency to contribute to a stable planar reflecting texture and the electric field effect which is to destroy this order by untwisting the helix. Finally and for higher voltages, the cell becomes transparent (e.g.: 218 V) when the structure is untwisted and free LC molecules are perpendicular to the electrodes. All the tested cells have similar electro-optical behaviours.

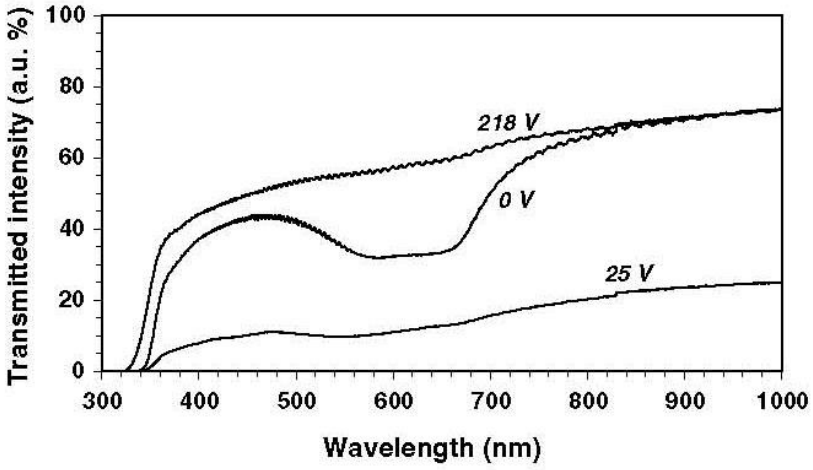

FIGURE 10. Transmittance spectra of a cell cured during a ramp from 70.3 to 35.4°C (exposure time = 60 min.) at zero volt (reflective state) and with 25 V (scattering state) and 218 V (transparent state) applied.

4. Discussion

On the broadening of the reflection band for the whole composite material when the polymer network is built under peculiar conditions, we first discuss the role of birefringence Δn and the pitch distribution p(z) (where z denotes the distance from the UV-exposed surface into the film) on $\Delta\lambda$. On the former point and from previous studies in conventional low molar mass CLCs[17 and references therein] and PSCLCs[18], we expect a decrease of refractive indices when the temperature is increased from the room cholesteric temperature until the isotropization point. If the network contributes 'to memorize' these variations, and due to the fact that the processes from high to low temperature are the most suitable conditions to increase $\Delta\lambda$, the evolution of Δn with temperature would play against larger $\Delta\lambda$. On Δn changes after curing, it has been shown that the extraordinary refractive index of the material raises upon polymerization[18]; this was attributed to the increase in the order parameter of the LC as a result of the increased clearing point upon polymerization. However, this modest

change in birefringence is not enough to explain a larger $\Delta\lambda$ upon peculiar out-of-equilibrium curing conditions. We have more to think to the presence of a pitch distribution p(z) within the gel and perhaps a pitch gradient as evidenced by scanning or transmission electron microscopy in polymeric[19, 20] and glassy[21-24] materials. Effectively, the blend pitch increases with the temperature (Fig. 3) and broadened $\Delta\lambda$ are obtained when the highest temperatures are included in the curing process. The fact that larger $\Delta\lambda$ are obtained in the case of ramps starting at high temperature/*large pitch* – close to 240 nm (Fig. 7.b) – by comparison with one-step processes at high temperature/*large pitch* – 190-200 nm (Fig. 5) – is in line with the hypothesis of cumulative effects in the phenomenon of broadening of reflection band. When the PSLC comes back to room temperature after curing, two different populations of low molar mass LC molecules experiment the phase transition[25]: one population behaves like the bulky LC and recovers the helical structure stable at room temperature whereas the other population is strongly bound to the network and adopts a structure which is very dependent on the non-reversible orientation of macromolecular network. In the present case, this fraction of bound LC molecules appears to be sufficient to introduce into the optical properties some reminiscence of the pitch variation which led to broadened bandwidthes. How to understand that $\Delta\lambda$ increase knows a sudden jump in temperature whereas the pitch is continuously varying? The characteristics of the phase separation between network-forming material and LC are temperature-dependent. The pores of the network at high temperature are usually described as larger than those at lower polymerization temperatures[15]. These changes in network morphology can be understood based upon kinetic model: the size of nodular beads (Fig. 8), and in turn, the final morphology, is determined by a balance between the rates of reaction and of bead diffusion. Under the hypothesis that $\Delta\lambda$ enlarged are due to an association of pitches assigned to the fraction of bound molecules and those assigned to the fraction of free molecules (with

intermediate situations corresponding to distorted pitches), this situation can be met when a minimum pore size in reached; if not, the fraction of free molecules regions could be too reduced in size. Enlarged $\Delta\lambda$ is the result of blends exhibiting large pitch from the beginning of the polymerization reaction with a sufficiently high temperature to control the parameters of phase separation like the pore size of the network.

5. Conclusion

PSCLCs have been elaborated by combining the UV-curing with a thermally-induced pitch variation. Different thermal processes were studied when the curing occurred during one single temperature of a continuous ramp for different times. $\Delta\lambda$ is tunable not by the chemistry of mesogens but by using a single blend and the right choice of thermal process. In relation with the pitch variation of the blend, $\Delta\lambda$ can be broadened by keeping constant the band position inside the spectrum ($\bar{\lambda}$ is not significantly shifted). These results display $\Delta\lambda$ close to 240 nm, for a peak centred around 620-630 nm, when current $\Delta\lambda$ for common cholesteric mixtures are typically between 80 and 100 nm at equivalent central wavelengths of the stop band. If some record was aimed for $\Delta\lambda$, CLC blends exhibiting a larger variety of reflection colors on a given temperature range would be used. It is shown that the functional materials are field-switchable: broadened reflective, scattering and transparent states are the main available modes when a cell is subjected to an increasing voltage; such a behaviour is similar to the conventional PSCLCs one. Broadening the light reflection band in CLCs and keeping the possibility to switch it by means of an electric field is relevant to switchable displays like white-or-black polarizer-free flat panels or smart windows to control the solar light spectrum by playing with the voltage.

Acknowledgements

The authors are grateful to Drs. F.-H. Kreuzer and E. Hanelt (Wacker Chemie GmbH) for their kind support and photocrosslinkable CLC compounds. This work was financed in part by the European Commission under the EESD Programme *Smart Win II* (ENK6-CT2001-00549). C. Rolland (Ecole des Mines, Albi-France) is acknowledged for her assistance in SEM investigations.

References

1. J. D. Joannopoulos, R. D. Meade, J. N. Winn, *Photonic Crystals: Molding the Flow of Light* (Princeton University Press, Princeton, 1995).

2. K. Sakoda, *Optical Properties of Photonic Crystals* (Springer Verlag, Berlin, 2001).

3. D. Dunmur and K. Toriyama, in *Physical Properties of Liquid Crystals*, edited by D. Demus, J. Goodby, G.W. Gray, H.-W. Spiess and V. Vill (Wiley-VCH, Weinheim, 1999), pp. 124-128.

4. For a review: I. Dierking, Adv. Mater. **12**, 167 (2000).

5. a) D.-K. Yang, L.-C. Chien, Y. K. Fung. b) H. Yuan, in *Liquid Crystals in Complex Geometries*, edited by G.P. Crawford and S. Zumer (Taylor and Francis, London, 1996), Ch. 5 and 12.

6. U. Behrens, H.–S. Kitzerow, Pol. Adv. Tech. **5**, 433 (1994).

7. S. Zumer and G. P. Crawford, in *Liquid Crystals in Complex Geometries*, edited by G. P. Crawford and S. Zumer (Taylor and Francis, London, 1996), Ch. 4.

8. H. Kikuchi, M. Yokota, Y. Hisakado, H. Yang, T. Kajiyama, Nature Materials **1**, 64 (2002).

9. F.-H. Kreuzer, D. Andrejewski, W. Haas, N. Häberle, G. Riepl and P. Spes, Mol. Cryst. Liq. Cryst. **199**, 345 (1991).

10. E. Nouvet and M. Mitov, Mol. Cryst. Liq. Cryst. **413**, 515 (2004).

11. a) R. Cano, Bull. Soc. Fr. Minér. Cryst. **90**, 333 (1967). b) R. Cano, Bull. Soc. Fr. Minér. Cryst. **91**, 20 (1968).

12. M. Mitov, A. Boudet, P. Sopéna and P. Sixou, Liq. Cryst. **23**, 903 (1997).

13. C. V. Rajaram, S. D. Hudson and L.-C. Chien, Chem. Mater. **7**, 2300 (1995).

14. F. Du and S.-T. Wu, Appl. Phys. Lett. **83**, 1310 (2003).

15. C. V. Rajaram, S. D. Hudson and L.-C. Chien, Chem. Mater. **8**, 2451 (1996).

16. D.-K. Yang, L.-C. Chien, J. W. Doane, Appl. Phys. Lett. **60**, 3102 (1992).

17. H. Kelker and R. Hatz, *Handbook of Liquid Crystals* (Verlag Chemie, Weinheim, 1980), pp. 330-332.

18. R. A. M. Hikmet and H. Kemperman, Liq. Cryst. **26**, 1645 (1999).

19. D. J. Broer, J. Lub and G. N. Mol, Nature **378**, 467 (1995).

20. A. Lavernhe, M. Mitov, C. Binet and C. Bourgerette, Liq. Cryst. **28**, 803 (2001).

21. M. Mitov, A. Boudet and P. Sopéna, Eur. Phys. J. B **8**, 327 (1999).

22. A. Boudet, C. Binet, M. Mitov, C. Bourgerette and E. Boucher, Eur. Phys. J. E **2**, 247 (2000).

23. M. Mitov, C. Binet, A. Boudet and C. Bourgerette, Mol. Cryst. Liq. Cryst. **358**, 209 (2001).

24. M. Mitov, C. Binet and C. Bourgerette in *Liquid Crystals V*, edited by I.-C. Khoo (Proc. of SPIE , 2001), vol. 4463, 11.

25. R. A. M. Hikmet, Mol. Cryst. Liq. Cryst. **198**, 357 (1991).